

Interpolating between Tikhonov regularization and spectral cutoff

Martin Sæbye Carøe¹, Mirza Karamehmedović¹, and Pierre Maréchal²

¹Department of Applied Mathematics and Computer Science, Technical University of Denmark, DK-2800 Kgs. Lyngby, Denmark

²Université Toulouse III - Paul Sabatier, 118 route de Narbonne, FR-31062 Toulouse, France

Abstract

Regularizing a linear ill-posed operator equation can be achieved by manipulating the spectrum of the operator's pseudo-inverse. Tikhonov regularization and spectral cutoff are well-known techniques within this category. This paper introduces an interpolating formula that defines a one-parameter family of regularizations, where Tikhonov and spectral cutoff methods are represented as limiting cases. By adjusting the interpolating parameter taking into account the specific operator equation under consideration, it is possible to mitigate the limitations associated with both Tikhonov and spectral cutoff regularizations. The proposed approach is demonstrated through numerical simulations in the fields of signal and image processing.

1 Introduction

We consider a general linear ill-posed operator equation

$$Tf = g, \quad (1)$$

in which $T: F \rightarrow G$ is a bounded linear operator from F to G , where F and G are infinite dimensional separable Hilbert spaces. In a number of real world applications, T is such that

$$\inf \{ \|Tf\| \mid f \in (\ker T)^\perp, \|f\| = 1 \} = 0. \quad (2)$$

When T is injective, an assumption which will be in force throughout, Condition (2) boils down to

$$\inf \{ \|Tf\| \mid \|f\| = 1 \} = 0. \quad (3)$$

The latter condition results in ill-posedness, meaning that:

- (i) the range $\text{ran } T$ of T is not closed in G ;
- (ii) the densely defined pseudo-inverse $T^\dagger: \text{ran } T + \ker T^* \rightarrow F$ is unbounded, so that the minimum-norm least squares solution to the linear equation $Tf = g$ does not depend continuously on the data g .

The purpose of regularization theory is to provide approximate solutions to (1) that depend continuously on the data, so as to avoid instability in the inversion process. See [1] and the references therein for a thorough treatment of regularization. The main objective of this paper is to bridge the gap between two of the most frequently used regularization methods, namely the Tikhonov regularization technique and the so-called spectral cutoff method. We shall propose a family of regularization techniques depending on some *interpolating parameter* that encompasses both Tikhonov regularization and the spectral cutoff as special (extreme) cases. The proposed filters can be naturally included in learning schemes [1] for further, data-driven refinement.

2 A family of regularization schemes

2.1 Spectral regularization

Prior to defining our interpolating family of regularization schemes, we establish a general theorem on spectral methods (see Theorem 2 below). This theorem is already well-known, but our approach to its proof is new in that we make use of the *singular value expansion* of general bounded operators. More precisely, we shall make use of the following theorem.

Theorem 1. Let $T: F \rightarrow G$ be an injective bounded linear operator, where F and G are real Hilbert spaces. There then exist

1. a Borel space $(\mathcal{M}, \mathcal{B}, \mu)$ with completely separable topology,
2. an unitary operator $V: L^2(\mathcal{M}, \mathcal{B}, \mu) \rightarrow F$ and an isometry $W: L^2(\mathcal{M}, \mathcal{B}, \mu) \rightarrow G$,
3. an essentially bounded measurable function $\sigma: \mathcal{M} \rightarrow \mathbb{R}$ that is strictly positive μ -almost everywhere, such that $T = W[\sigma]V^*$, in which $[\sigma]$ denotes the operator of multiplication by σ . Moreover, $\text{ran } W = \overline{\text{ran } T}$.

See [5, Theorem 3]. The following diagram illustrates the singular value expansion exhibited in the last theorem:

$$\begin{array}{ccc} F & \xrightarrow{T} & G \\ \uparrow V & & \uparrow W \\ L^2(\mathcal{M}, \mathcal{B}, \mu) & \xrightarrow{[\sigma]} & L^2(\mathcal{M}, \mathcal{B}, \mu) \end{array}$$

Under Condition (3), $\text{ran } T$ is not closed. By [5, Theorem 4], this implies that σ is not bounded away from zero. On the other hand, since $\text{ran } W = \overline{\text{ran } T}$,

$$\ker T^* = (\text{ran } W)^\perp = \ker W^*.$$

Clearly, the injectivity of T implies that of W , which in turn implies that $W^\dagger = (W^*W)^{-1}W^* = W^*$. As can be easily seen, the following factorizations hold:

$$\begin{aligned} T^* &= V[\sigma]W^*, \\ T^*T &= V[\sigma^2]V^*, \\ T^\dagger = (T^*T)^{-1}T^* &= V[\sigma^{-1}]W^*. \end{aligned}$$

Recall that a family (R_α) of bounded operators from G to F is said to be a *regularization of T^\dagger* if there exists a *parameter choice rule*

$$\begin{aligned} \alpha: \quad \mathbb{R}_+ \times G &\longrightarrow \mathbb{R}_+ \setminus \{0\} \\ (\delta, g^\delta) &\longmapsto \alpha(\delta, g^\delta) \end{aligned}$$

such that

- (1) $\sup \{ \|\alpha(\delta, g^\delta)\| \mid g^\delta \in G, \|g^\delta - g\| \leq \delta \} \rightarrow 0$ as $\delta \downarrow 0$;
- (2) $\sup \{ \|R_{\alpha(\delta, g^\delta)}g^\delta - T^\dagger g\| \mid g^\delta \in G, \|g^\delta - g\| \leq \delta \} \rightarrow 0$ as $\delta \downarrow 0$;

Recall also that (R_α) is a regularization of T^\dagger if (R_α) converges pointwise to T^\dagger on its domain

$$\mathcal{D}(T^\dagger) = \text{ran } T + (\text{ran } T)^\perp = \text{ran } T + \ker T^*.$$

See [6, Proposition 3.4].

The following result is well-known; however, we here propose a novel proof:

Theorem 2. Let $T: F \rightarrow G$ be an injective bounded operator with singular value expansion $T = W[\sigma]V^*$ as in Theorem 1. Assume that σ is not bounded away from zero, so that the inverse problem $Tf = g$ is ill-posed. Let $q: \mathbb{R}_+^* \times \mathbb{R}_+ \rightarrow \mathbb{C}$ be such that

- (A1) for every $(\alpha, \sigma) \in \mathbb{R}_+^* \times \mathbb{R}_+$, $|q(\alpha, \sigma)| \leq M$ for some positive constant M ,
- (A2) for every $\sigma \in \mathbb{R}_+$, $|q(\alpha, \sigma)| \leq c_\alpha \sigma$, in which c_α is some positive constant.

Then $R_\alpha := V[\sigma^{-1}q(\alpha, \sigma)]W^*$ is well-defined and bounded, and $\|R_\alpha\| \leq c_\alpha$. Moreover, if

(A3) for every $\sigma \in \mathbb{R}_+$, $\lim_{\alpha \downarrow 0} q(\alpha, \sigma) = 1$,

then (R_α) is a regularization of T^\dagger .

Proof. Let $g \in \mathcal{D}(T^\dagger)$ and let \bar{g} be its projection onto the closure of the range of T . Observe that, since g belongs to the domain of T^\dagger , its projection \bar{g} must actually belong to the range of T . Hence $\bar{g} = Tf$ for some $f \in F$, from which we deduce that

$$[\sigma^{-1}]W^*\bar{g} = [\sigma^{-1}]W^*W[\sigma]V^*f = V^*f \in L^2(\mathcal{M}, \mathcal{B}, \mu).$$

By Assumption (A1), $[q(\alpha, \sigma)][\sigma^{-1}]W^*g = [q(\alpha, \sigma)]V^*f$ also belongs to $L^2(\mathcal{M}, \mathcal{B}, \mu)$, which in turn implies that

$$V[q(\alpha, \sigma)][\sigma^{-1}]W^*g =: R_\alpha g$$

is well-defined. Under Assumption (A2), we have, for every $g \in G$,

$$\begin{aligned} \|R_\alpha g\|^2 &= \|V[\sigma^{-1}q(\alpha, \sigma)]W^*g\|^2 \\ &= \|[\sigma^{-1}q(\alpha, \sigma)]W^*g\|^2 \\ &\leq \|\sigma^{-1}q(\alpha, \sigma)\|_\infty^2 \|W^*g\|^2 \\ &= \|\sigma^{-1}q(\alpha, \sigma)\|_\infty^2 \|g\|^2 \\ &\leq c_\alpha^2 \|g\|^2, \end{aligned}$$

in which the second equality is due to the unitarity of V and the third equality is due to the fact that W is an isometry (so that $W^*W = I$, where I denotes the identity). The first assertion in the theorem follows.

Next, let $f^\dagger := T^\dagger g$ and $f_\alpha := R_\alpha g$. From the definition of R_α and the formula for T^\dagger , we readily see that

$$f^\dagger - f_\alpha = V[\sigma^{-1}(1 - q(\alpha, \sigma))]W^*g = V[1 - q(\alpha, \sigma)][\sigma^{-1}]W^*\bar{g} = V[1 - q(\alpha, \sigma)]V^*f.$$

Therefore, using the unitarity of V ,

$$\|f^\dagger - f_\alpha\|^2 = \|[1 - q(\alpha, \sigma)]V^*f\|_{L^2(\mathcal{M}, \mathcal{B}, \mu)}^2 = \int |1 - q(\alpha, \sigma)|^2 (V^*f(\sigma))^2 d\mu(\sigma).$$

Finally, under Assumption (A3), the function $\sigma \mapsto |1 - q(\alpha, \sigma)|^2$ converges pointwise to zero, and Lebesgue's dominated convergence theorem then implies that $f_\alpha \rightarrow f^\dagger$ as $\alpha \downarrow 0$. \square

Notice that in the above theorem, q is allowed to take complex values. Notice also that $q(\alpha, \cdot)$ need only be defined on the range of σ .

The latter theorem generalizes Theorem 4.9 in [4], in which compactness of T was assumed. This special case now appears as a corollary. If we let T be a compact operator, then the singular value expansion takes the form

$$Tx = \sum_{n=1}^{\infty} \sigma_n(g_n \otimes f_n)f = \sum_{n=1}^{\infty} \sigma_n \langle f_n, f \rangle g_n,$$

in which the σ_n are the so-called singular values, (f_n) is a Hilbert basis of F and (g_n) is a Hilbert basis of $\overline{\text{ran } T}$. This is a particular case of Theorem 1, in which the Borel space is $l^2_{\mathbb{R}}$, the space of square summable real sequences, endowed with the counting measure. It can be easily checked that the operators W and V are respectively given in this case by

$$W(s_n) = \sum_{n=1}^{\infty} s_n g_n \quad \text{and} \quad V(s_n) = \sum_{n=1}^{\infty} s_n f_n.$$

Theorem 2 then takes the following form:

Corollary 1. Let $T: F \rightarrow G$ be an injective compact operator with singular value expansion $T = \sum_{n=1}^{\infty} \sigma_n(g_n \otimes f_n)$. Let $q: \mathbb{R}_+^* \times \{\sigma_n | n \in \mathbb{N}^*\} \rightarrow \mathbb{C}$ be such that

(A1) for every $\alpha \in \mathbb{R}_+^*$ and every $n \in \mathbb{N}^*$, $|q(\alpha, \sigma_n)| \leq M$ for some positive constant M ,

(A2) for every $n \in \mathbb{N}^*$, $|q(\alpha, \sigma_n)| \leq c_\alpha \sigma_n$, in which c_α is some positive constant.

Then $R_\alpha := \sum_{n=1}^{\infty} \sigma_n^{-1} q(\alpha, \sigma_n) (f_n \otimes g_n)$ is well-defined and bounded, and $\|R_\alpha\| \leq c_\alpha$. Moreover, if

(A3) for every $n \in \mathbb{N}^*$, $\lim_{\alpha \downarrow 0} q(\alpha, \sigma_n) = 1$,

then (R_α) is a regularization of T^\dagger .

An important example of an ill-posed inverse problem is the standard deconvolution problem. Given a function γ in $L^1(\mathbb{R}^n)$, we consider the convolution operator $T_\gamma : L^2(\mathbb{R}^n) \rightarrow L^2(\mathbb{R}^n)$ defined by

$$T_\gamma f = \gamma * f.$$

The deconvolution problem consists in solving $T_\gamma f = g$ for f when g is empirically known. This problem is ubiquitous in many areas of applied sciences, including signal and image processing, physics, statistics etc. If γ has an almost everywhere positive-valued Fourier transform $\hat{\gamma}$ then the singular value expansion is explicit:

$$T_\gamma = W[\hat{\gamma}]V^* \quad \text{with} \quad W = V = U^{-1}$$

where $U : L^2(\mathbb{R}^n) \rightarrow L^2(\mathbb{R}^n)$ is the Fourier-Plancherel operator. Recall that the Fourier-Plancherel operator can be defined as the closure to $L^2(\mathbb{R})$ of the Fourier transform, denoted likewise, on $L^1(\mathbb{R}^n) \cap L^2(\mathbb{R}^n)$. Our definition of the Fourier transform of an integrable function f on \mathbb{R}^n is:

$$(Uf)(\xi) = \hat{f}(\xi) := \int_{\mathbb{R}^n} f(x) e^{-2\pi i \langle x, \xi \rangle} dx.$$

Under the standard assumption that $\text{meas}\{\xi \in \mathbb{R}^n | \hat{\gamma}(\xi) = 0\} = 0$ the operator T_γ is injective. Remember that by the Riemann-Lebesgue lemma, $\hat{\gamma}$ is continuous and vanishes at infinity, which implies (via [5, Theorem 4]) that the deconvolution problem is ill-posed. This particular situation is illustrated below:

$$\begin{array}{ccc} L^2(\mathbb{R}^n) & \xrightarrow{T_\gamma} & L^2(\mathbb{R}^n) \\ \uparrow_{U^{-1}} & & \uparrow_{U^{-1}} \\ L^2(\mathbb{R}^n) & \xrightarrow{[\hat{\gamma}]} & L^2(\mathbb{R}^n) \end{array}$$

The last example reveals potential drawbacks of both Tikhonov regularization and the spectral cutoff. Recall that the variational formulation of the Tikhonov regularization consists in the minimization of the functional

$$\mathcal{F}(f) = \|g - T_\gamma f\|^2 + \|f\|^2 = \|\hat{g} - \hat{\gamma}\hat{f}\|^2 + \|\hat{f}\|^2,$$

where we used Parseval's identity. We see that the penalty term acts with equal strength everywhere in the Fourier domain. This can't be optimal since the *low frequencies* are constrained by the data, $\hat{\gamma}$ being close to 1 near the origin (Charibdis). On the other hand, the spectral cutoff multiplies the Fourier transform of f by a *mask*, which is equivalent to convolving f by a sinc-like function, thereby creating the Gibbs phenomenon (Sylla).

Our intuition is that we may somehow find a reasonable compromise placing us in between these two choices for q . In the next subsection, we propose an interpolation formula for the function q , and show that it fits the regularization framework of Theorem 2. Later on, we shall determine optimal values for the interpolating parameter. Finally, we shall illustrate the performance of our new family of regularization schemes by means of numerical simulation.

2.2 Interpolating between Tikhonov and spectral cutoff

Two important special cases of the function q that appears in Theorem 2 are

$$q_0(\alpha, \sigma) = \frac{\sigma^2}{\alpha + \sigma^2} \quad \text{and} \quad q_\infty(\alpha, \sigma) = \begin{cases} 1 & \text{if } \sigma > \sqrt{\alpha}, \\ 1/2 & \text{if } \sigma = \sqrt{\alpha}, \\ 0 & \text{if } \sigma < \sqrt{\alpha}. \end{cases}$$

The function q_0 corresponds to Tikhonov regularization. It satisfies (A1), (A2) and (A3) with $M = 1$ and $c_\alpha = \frac{1}{2\sqrt{\alpha}}$. The function q_∞ corresponds to spectral cutoff. It satisfies (A1), (A2) and (A3) with $M = 1$ and $c_\alpha = \frac{1}{\sqrt{\alpha}}$.

We now define the family $(q_\tau)_{\tau \in \mathbb{R}_+}$ by

$$q_\tau(\alpha, \sigma) = \frac{1}{1 + \left(\frac{\sqrt{\alpha}}{\sigma}\right)^{2+\tau}}. \quad (4)$$

It is readily seen that $\tau = 0$ yields the Tikhonov case while in the limit $\tau \rightarrow \infty$ one retrieves the spectral cutoff case.

As can be seen in Figure 1, the filter functions q_τ operate somewhere in-between the Tikhonov regularization and TSVD by making the cut-off around $\sqrt{\alpha}$ more steep than for the Tikhonov regularization, but less steep than the TSVD.

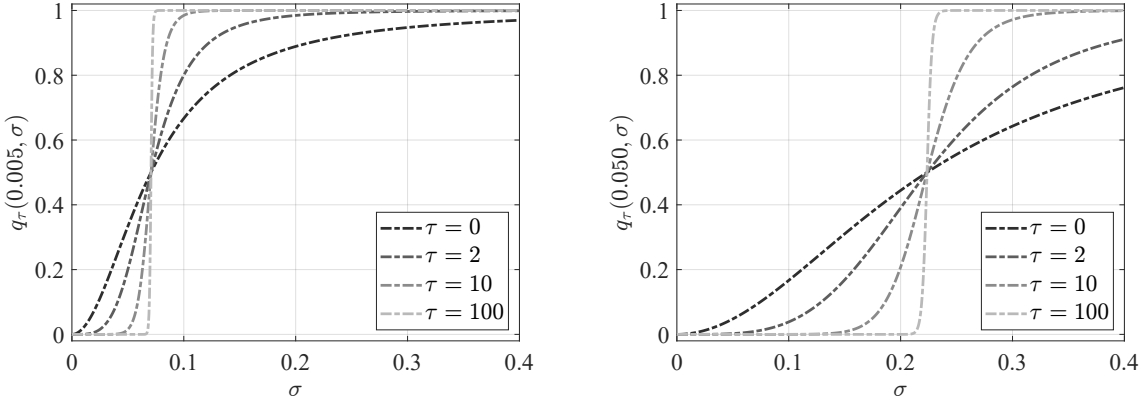


Figure 1: A plot of q_τ with $\alpha = 0.005$ (left) and $\alpha = 0.05$ (right) and four different values of τ .

The above function q_τ corresponds to the minimization of the functional

$$f \mapsto \frac{1}{2} \|g - Tf\|^2 + \frac{1}{2} \|H_\alpha f\|^2, \quad (5)$$

in which H_α is the closed operator on F given by

$$H_\alpha = V \left[\sqrt{\alpha} \left(\frac{\sqrt{\alpha}}{\sigma} \right)^{\tau/2} \right] V^*.$$

The closedness of H_α guarantees the existence and uniqueness of solution of the minimization problem (5). [10, Theorem 1 on p. 3]

As a matter of fact, using the expansion $T = W[\sigma]V^*$, we then have (see [10, Section 25, p. 214]):

$$\begin{aligned} f_\alpha &= (T^*T + H_\alpha^* H_\alpha)^{-1} T^* g \\ &= \left(V[\sigma^2] V^* + V \left[\alpha \left(\frac{\sqrt{\alpha}}{\sigma} \right)^\tau \right] V^* \right)^{-1} V[\sigma] W^* g \\ &= V \left[\frac{1}{\sigma} \frac{\sigma^2}{\sigma^2 + \alpha \left(\frac{\sqrt{\alpha}}{\sigma} \right)^\tau} \right] W^* g \\ &= V \left[\frac{1}{\sigma} q_\tau(\alpha, \sigma) \right] W^* g, \end{aligned}$$

with q_τ as in (4). We stress here that the operator H_α depends both on α and the function σ . Its closedness is established in Appendix A. In a number of cases, including the deconvolution problem considered in the previous subsection, σ is explicitly known, so that the dependence of H_α on σ is not an obstacle. We also emphasize that, strictly speaking, the above regularization does not pertain to the so-called *generalized Tikhonov* class. As a matter of fact, the dependence of H on α is not that one would have if α was merely a weight in front of some α -independent quadratic penalty in the objective functional displayed in (5).

3 Numerical examples

We test the family of regularization schemes on a 1D deconvolution problem. Recall that the operator $T_\gamma: L^2(\mathbb{R}) \rightarrow L^2(\mathbb{R})$ of convolution by $\gamma \in L^1(\mathbb{R})$ is given by $T_\gamma = \gamma * f$. It can be diagonalized by the Fourier-Plancherel operator.

Let $\mathbf{f}, \gamma \in \mathbb{R}^n$ with $n \in \mathbb{N}$ be samples of functions f, γ in $L^2(\mathbb{R})$ and $L^1(\mathbb{R})$, respectively. We assume that the support of f and γ is contained in the interval $[-1, 1]$, and that the samples are taken at a uniform grid in this box. We can compute the discrete convolution to obtain $\mathbf{g} \in \mathbb{R}^n$, given by

$$g_j = \sum_{j'=1}^n f_{j-j'} \gamma_{j'} h, \quad (6)$$

where \mathbf{f} and γ are extended by zero to all indices $j \notin \{1, \dots, n\}$, and where h is the spacing between points on the grid.

Note that the discrete convolutions (6) correspond to the Riemann sum approximations to the continuous convolution.

Consider a noisy measurement $\mathbf{g} \in \mathbb{R}^n$. We compute reconstructions $\mathbf{f}_{\alpha, \tau} \in \mathbb{R}^n$ by computing

$$\mathbf{f}_{\alpha, \tau} = U^{-1} \left(\frac{1}{U\gamma} q_\tau(\alpha, U\gamma) \right) U\mathbf{g}. \quad (7)$$

Here $U: \mathbb{R}^n \rightarrow \mathbb{R}^n$ is a linear operator that approximates the continuous Fourier transform. The discrete Fourier transform operator can be used to approximate the Fourier transform, as shown in [2].

For the 2D example, we will consider the Shepp-Logan phantom, a piece-wise constant grey-scale image with values between 0 and 1. We convolve f with a kernel that is equal to the characteristic function times a scalar multiple. In particular, $\gamma = c \cdot \chi_A$, where $c > 0$ is chosen such that $\int_A \gamma(x) dx = 1$. In the numerical example, $A = [-s_{\text{blur}}, s_{\text{blur}}]$, for some number $s_{\text{blur}} > 0$.

3.1 1D example

We consider three different functions $f^i: \mathbb{T} \rightarrow [0, 1]$, $i = 1, 2, 3$, where $\mathbb{T} = [-1, 1]$ is the 1-dimensional torus, which identifies the elements -1 and 1 .

The first function f^1 is continuous and piecewise smooth. The function f^2 has one discontinuity. The function f^3 is C^∞ . All three functions are shown in the top left of Figures 2, 3 and 4, respectively.

The (exact) convolutions $g^i = \gamma * f^i$ are computed and sampled on a uniform grid $x_j = -1 + 2j/N$, $j = 0, 1, \dots, N-1$ to obtain the exact measurements $g_j^i = g^i(x_j)$. Random Gaussian i.i.d. noise, ε_j^σ with standard deviation $\sigma > 0$ is added to obtain a noisy measurement $\mathbf{g}^{i, \sigma} = [g_j^i + \varepsilon_j^\sigma]$. In the implementation the "exact" measurement g_j is in fact computed using a discrete convolution on a much finer grid than the grid (x_j) . As explained, reconstructions are computed using Equation (7), where U is an approximation to the Fourier transform using the discrete Fourier transform.

The error in the reconstruction, relative to the true signal f^i , is computed by

$$\|\mathbf{f}_{\alpha, \tau}^i - \mathbf{f}^i\|_2 / \|\mathbf{f}^i\|_2,$$

where $\mathbf{f}^i = [f^i(x_j)]$.

The values of α are chosen in two different ways:

- The *Morozov principle* [10]: α is chosen as

$$\alpha = \sup\{a' > 0 : \|\gamma * \mathbf{f}_{\alpha, \tau} - \mathbf{g}^\sigma\|_2 \leq 1.1 \cdot \mathbb{E}(\|\varepsilon\|_2)\}.$$

where the expected value of the norm of the error is $\mathbb{E}(\|\varepsilon\|_2) = \sigma\sqrt{N}$.

- Optimal choice: α is found by running through a large collection of values and choosing the value of $\alpha > 0$ that gives the lowest reconstruction error $\|\mathbf{f}_{\alpha, \tau}^i - \mathbf{f}^i\|_2 / \|\mathbf{f}^i\|_2$.

The results of the experiment are shown in Figure 2, 3, 4 and Table 1, 2 and 3.

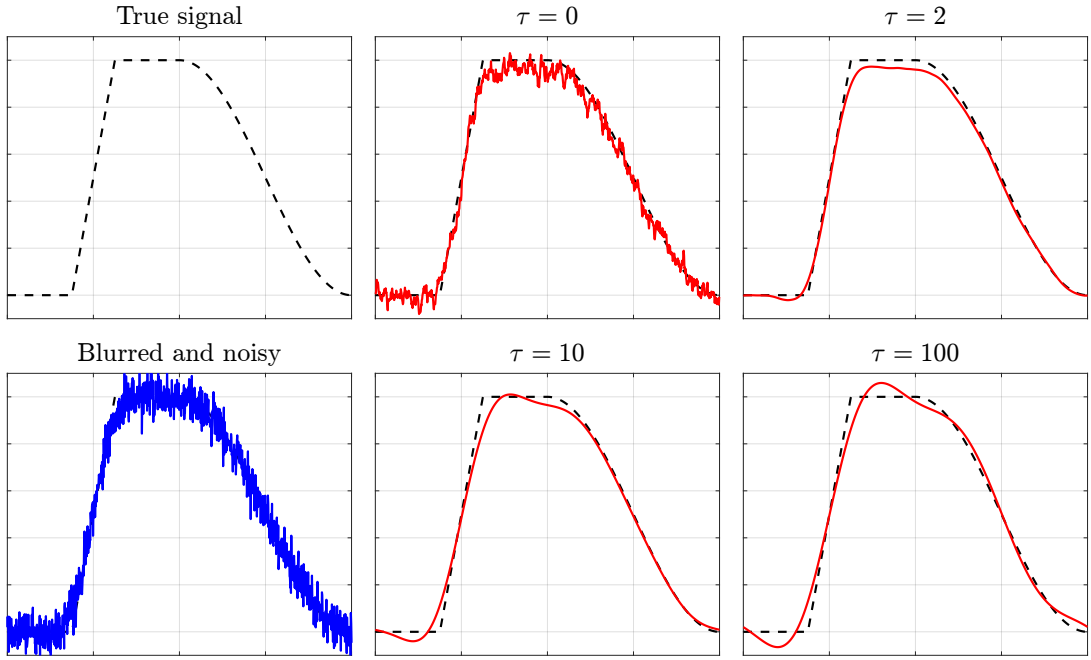


Figure 2: Reconstruction of f^1 . Here we set $s_{\text{blur}} = 0.1$, $N = 1001$ and noise level $\sigma = 0.05$, and α is determined using the Morozov principle.

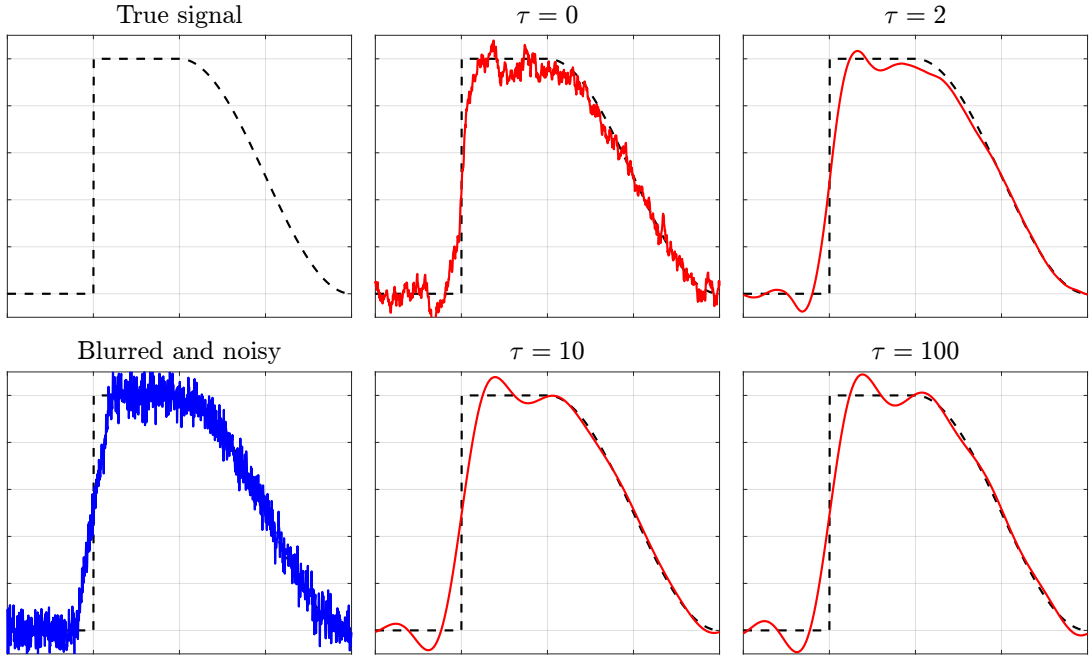


Figure 3: Reconstruction of f^2 . Here we set $s_{\text{blur}} = 0.1$, $N = 1001$ and noise level $\sigma = 0.05$, and α is determined using the Morozov principle.

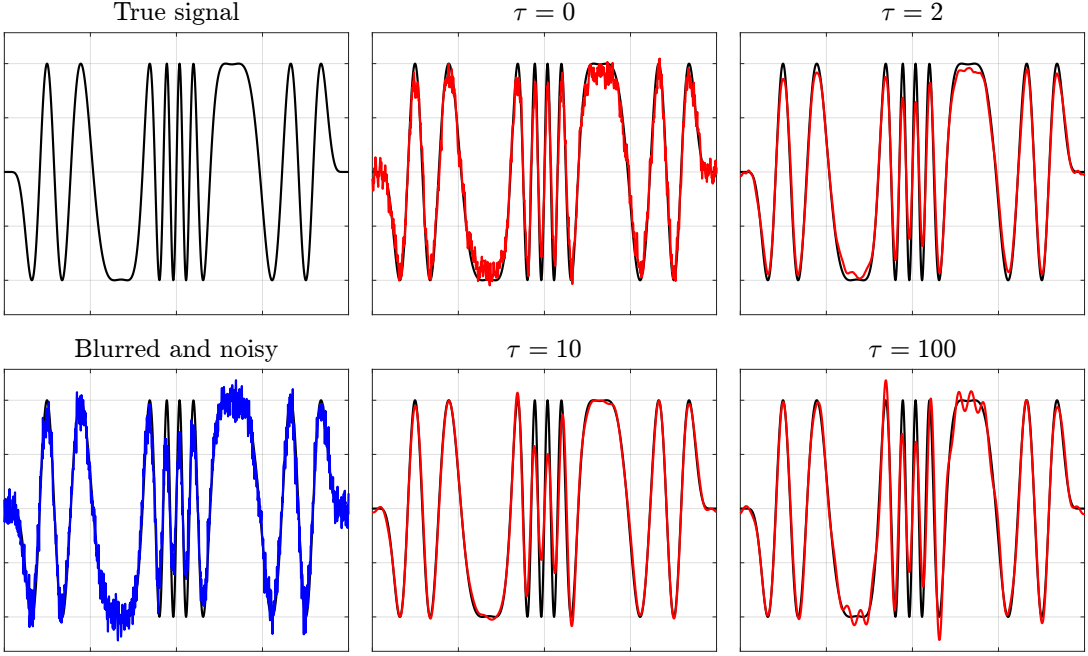


Figure 4: Reconstruction of f^3 . Here we set $s_{\text{blur}} = 0.03$, $N = 1001$ and noise level $\sigma = 0.075$, and α is found using the Morozov principle.

		$\tau = 0$	$\tau = 2$	$\tau = 10$	$\tau = 100$
Morozov principle	Error	0.0615	0.0364	0.0471	0.0559
Morozov principle	α	0.0354	0.1727	0.5032	0.5620
Optimal choice	Error	0.0607	0.0192	0.0193	0.0194
Optimal choice	α	0.0417	0.0753	0.1239	0.1286

Table 1: Reconstruction of f^1 . Here we set $s_{\text{blur}} = 0.1$, $N = 1001$ and noise level $\sigma = 0.05$.

		$\tau = 0$	$\tau = 2$	$\tau = 10$	$\tau = 100$
Morozov principle	Error	0.1154	0.1288	0.1403	0.1413
Morozov principle	α	0.0328	0.1490	0.2841	0.2497
Optimal choice	Error	0.1154	0.1037	0.1081	0.1098
Optimal choice	α	0.0317	0.0192	0.0236	0.0258

Table 2: Reconstruction of f^2 . Here we set $s_{\text{blur}} = 0.1$, $N = 1001$ and noise level $\sigma = 0.05$.

		$\tau = 0$	$\tau = 2$	$\tau = 10$	$\tau = 100$
Morozov principle	Error	0.1585	0.1355	0.1621	0.1821
Morozov principle	α	0.0873	0.2277	0.3354	0.3354
Optimal choice	Error	0.1577	0.0861	0.0779	0.0777
Optimal choice	α	0.0811	0.0993	0.1012	0.0889

Table 3: Reconstruction of f^3 . Here we set $s_{\text{blur}} = 0.03$, $N = 1001$ and noise level $\sigma = 0.075$.

We clearly see that Tikhonov regularization ($\tau = 0$), does not remove all the oscillations of the noise. On the other hand, with $\tau = 100$, meaning almost spectral cutoff, we see large oscillations close to discontinuities or regions with rapid changes in the function value. Depending on the method for choosing α , choosing an intermediate value of τ (for example $\tau = 2$ or $\tau = 10$) somewhat removes these two drawbacks of Tikhonov regularization and spectral cutoff.

Regardless of the value of τ , the regularization methods fails to reconstruct the function accurately at discontinuities or in regions with rapid changes in the function value.

3.2 2D example

We consider the multi-frequency inverse source problem in two dimensions. Let $D_0, D \subset \mathbb{R}^2$ be concentric disks with radii R_0, R satisfying $R_0 < R$, and let D_0 include the support of an unknown acoustic or electromagnetic source function $s \in L^2(D_0)$. For each wavenumber ('frequency') $k > 0$, the field u_k radiated by s satisfies the Helmholtz equation

$$(\Delta + k^2)u_k(x) = s(x), \quad x \in \mathbb{R}^2, \quad (8)$$

together with the Sommerfeld radiation condition

$$\lim_{|x| \rightarrow \infty} \sqrt{|x|}(\partial_{|x|} - ik)u_k(x) = 0, \quad \text{uniformly for } x/|x| \in S^1. \quad (9)$$

The measured data are given by the restriction of u_k to the boundary ∂D . The corresponding forward operator $F_k : s \mapsto U_k := u_k|_{\partial D}$, compact from $L^2(D_0)$ to $L^2(\partial D)$, is given by the radiation integral

$$U_k(x) = (F_k s)(x) = \int_{y \in D_0} \Phi_k(x - y)s(y)dy, \quad x \in \partial D, \quad (10)$$

where $\Phi_k(x) = \frac{i}{4}H_0^{(1)}(k|x - y|)$ is the outgoing fundamental solution of the Helmholtz equation in the plane, and $H_0^{(1)}$ is the Hankel function of order zero and of first kind. A singular value expansion of F_k was given and characterized in [7]; see also [3]. For a set of frequencies $Q = \{k_j\}_{j \in I}$ and corresponding boundary measurements $\{U_{k_j}\}$, the multi-frequency inverse source problem is to reconstruct $s \in L^2(D_0)$ such that

$$U_{k_j} = F_{k_j} s, \quad \forall k_j \in Q. \quad (11)$$

The inverse source problem is ill-posed since $\ker F_k = (\Delta + k^2)H^2(D_0)$. [9] The degree of ill-posedness of the inverse problem depends on the choice of the frequency set Q [8], with broader frequency coverage leading to a larger subspace of source functions that can be reconstructed in a stable manner.

For the numerical experiment, we discretize the domain D using a triangular mesh, generate a synthetic ground truth source s , and compute boundary data using the forward operator (10). For this experiment we select the frequencies k_j according to

$$k_j R_0 = j\pi, \quad j = 2, \dots, 30. \quad (12)$$

We assemble the individual-frequency discretized forward operators into a single joint system matrix and compute its singular value decomposition. Finally, we reconstruct the source using the spectral filtering method defined in (7). Our code is available at https://github.com/msaca-okse/tikhonov_ISP.

Figure 5 shows the ground truth (top left) and reconstructions corresponding to different values of τ . Figure 6 shows the singular value spectrum of the combined forward operator (all used frequencies) together with the projections of the ground truth onto the corresponding right singular vectors. We clearly see that neither the Tikhonov regularization ($\tau = 0$) nor the truncated SVD regularization (τ large) give the best solution of the inverse source problem, in that the first includes speckle-like artifacts and the latter exhibits the Gibbs phenomenon near the piecewise constant component of the source. In fact, the choice $\tau = 3$ seems to be better than both of the extreme options.

A Appendix: Closedness of the operator H_α

We may consider the operator $H = H_1$, since the positive constant $(\sqrt{\alpha})^{1+\tau/2}$ doesn't play any role:

$$H = V \left[\sigma^{-\tau/2} \right] V^*.$$

Recall that $V : L^2(\mathcal{M}, \mathcal{B}, \mu) \rightarrow F$ is unitary. If $\phi \in \text{ran } H$, then $H^{-1}\phi = V \left[\sigma^{\tau/2} \right] V^* \phi$. It is readily seen that the domain of H is given by

$$\mathcal{D}(H) = \left\{ f \in F \mid \sigma^{-\tau/2} V^* f \in L^2(\mathcal{M}, \mathcal{B}, \mu) \right\}.$$

Now assume that $f_n \in \mathcal{D}(H)$, that $f_n \rightarrow f$, and $Hf_n \rightarrow \varphi$ in F . We have:

$$\begin{aligned} \varphi = \lim Hf_n \text{ in } F &\Leftrightarrow V^* \varphi = \lim V^* Hf_n \text{ in } L^2(\mathcal{M}, \mathcal{B}, \mu) \\ &\Leftrightarrow [\sigma(x)^{\tau/2}] V^* \varphi = \lim [\sigma(x)^{\tau/2}] V^* Hf_n \text{ in } L^2(\mathcal{M}, \mathcal{B}, \mu) \\ &\Leftrightarrow V \left[\sigma(x)^{\tau/2} \right] V^* \varphi = \lim V \left[\sigma(x)^{\tau/2} \right] V^* Hf_n \text{ in } F, \end{aligned}$$

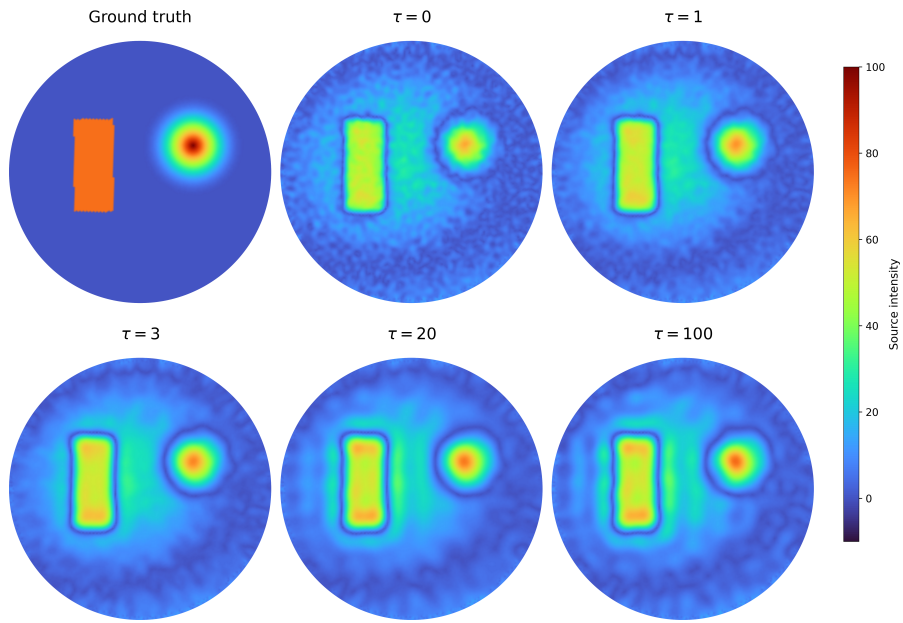


Figure 5: The ground truth (top left) and reconstructions for different values of τ . We set D to be the unit disc, and D_0 to be the disc centered at the origin with radius 0.99.

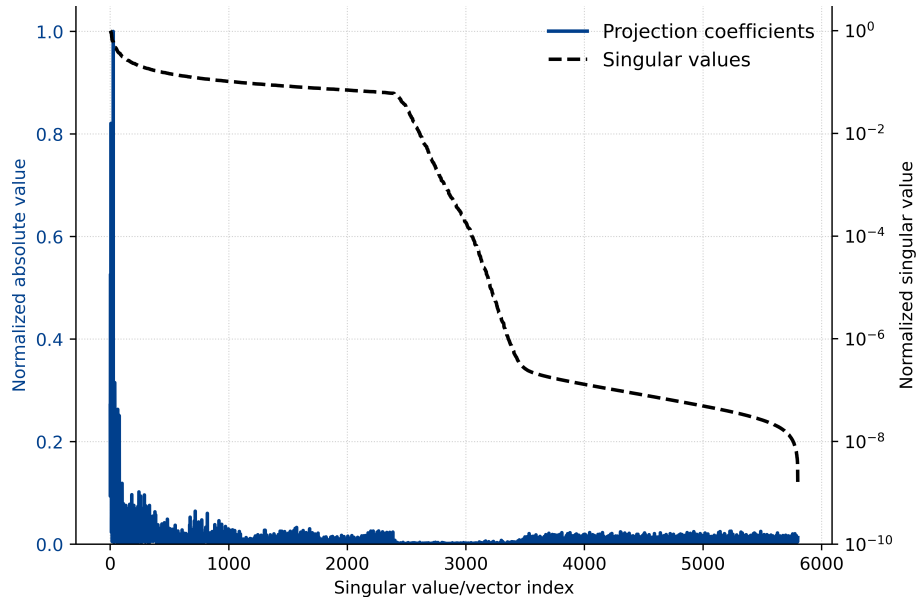


Figure 6: The singular value spectrum of the combined forward operator, with projections of the ground truth onto the corresponding right singular vectors.

in which the first and third equivalence stem from the unitarity of V , while the second equivalence follows from the boundedness of the function $\sigma(x)^{\tau/2}$. Therefore, since $Hf_n \in \text{ran } H$ and $V[\sigma(x)^{\tau/2}]V^* = H^{-1}$, we obtain that $f = H^{-1}\varphi$, which implies in turn that $f \in \mathcal{D}(H)$ and $Hf = \varphi$. As a matter of fact,

$$\begin{aligned} \int \sigma(x)^{-\tau} |(V^*f)(x)|^2 d\mu(x) &= \int \sigma(x)^{-\tau} |V^*H^{-1}\varphi(x)|^2 d\mu(x) \\ &= \int \sigma(x)^{-\tau} \sigma(x)^\tau |V^*\varphi(x)|^2 d\mu(x) \\ &= \int |V^*\varphi(x)|^2 d\mu(x), \end{aligned}$$

the last integral being finite since $V^*\varphi \in L^2(\mathcal{M}, \mathcal{B}, \mu)$. This proves the closedness of H .

References

- [1] Simon Arridge, Peter Maass, Ozan Öktem, and Carola-Bibiane Schönlieb, *Solving inverse problems using data-driven models*, Acta Numerica (2019), 1–174.
- [2] David H. Bailey and Paul N. Swarztrauber, *A Fast Method for the Numerical Evaluation of Continuous Fourier and Laplace Transforms*, SIAM Journal on Scientific Computing **15** (1994), no. 5, 1105–1110.
- [3] G. Bao, J. Lin, and F. Triki, *A multi-frequency inverse source problem*, Journal of Differential Equations **249** (2010), no. 12, 3443–3465.
- [4] David L. Colton and Rainer Kress, *Inverse acoustic and electromagnetic scattering theory*, 4nd ed., Springer, 2013.
- [5] Daniel K Crane and Mark S Gockenbach, *The singular value expansion for arbitrary bounded linear operators*, Mathematics **8** (2020), no. 8, 1346.
- [6] Heinz Werner Engl, Martin Hanke, and Andreas Neubauer, *Regularization of inverse problems*, vol. 375, Springer Science & Business Media, 1996.
- [7] Mirza Karamehmedović, *Explicit tight bounds on the stably recoverable information for the inverse source problem*, Journal of Physics Communications **2** (2018), no. 095021.
- [8] Mirza Karamehmedović, Adrian Kirkeby, and Kim Knudsen, *Stable source reconstruction from a finite number of measurements in the multi-frequency inverse source problem*, Inverse Problems **34** (2018), no. 6, 065004.
- [9] Edwin A. Marengo and Richard W. Ziolkowski, *On the Radiating and Nonradiating Components of Scalar, Electromagnetic, and Weak Gravitational Sources*, Physical Review Letters **83** (1999), no. 17.
- [10] V.A. Morozov, *Methods for Solving Incorrectly Posed Problems*, Springer, 1984.